The Stationary Soliton Molecules Generation and Management in Tm-Doped Mode-Locked Fiber Oscillator

Shaohui Mo, Peilong Yang, Kai Xia, Meng Lv, Shengchuang Bai, Peipeng Xu, Qiuhua Nie, and Shixun Dai

Abstract— **We present an investigation on the high-SNR stationary soliton molecules generation and its characteristics analysis in a Tm-doped nonlinear polarization rotation (NPR) mode-locked laser oscillator. By inserting a narrow band filter, we successfully improved the generated soliton molecules with signal-to-noise ratio (SNR) to above 80 dB. This value is the highest ever reported to the best of our knowledge. In addition, we also explored the details of the temporal and spectral evolution of the generated solitons while optimizing the related parameters, including pump power, waveplates, intracavity dispersion, and so on. Such stationary soliton molecules with many interesting features will find many applications in high-speed telecommunications and micro-processing.**

Index Terms— **Fiber laser, soliton molecules, Tm-doped fiber.**

I. INTRODUCTION

IN THE last decade, passively mode-locked fiber lasers around 2-μm "eye safe" regions have attracted much attention due to their unmatched practical applications in fields such as surgery, spectroscopy, high-precise metrology, atmospheric remote sensing, and environmental monitoring. With the development of ultrafast lasers, researches on the passively mode-locking phenomenon in cavities have led to the discoveries of some fascinating results in soliton dynamics, such as soliton molecules, vector solitons, soliton explosions, soliton rain in the same dissipative system [1]. In addition, the advent of new styled fibers promoted the development of fiber communications in a 2 μm band [2]. In fiber communication system, following the entropy flow considerations, the rate of information flow through the channel depends on the channel capacity, which is set by the SNR or the coding format more suitable for digital transmission [3]. To extend the coding alphabet, soliton molecules are considered as an available solution. In addition to the single-mode fiber has a stronger anomalous dispersion at 2 μm, which facilitates the generation of soliton molecules with more complex structure for exploration.

Since Tang et al. firstly reported the observation of soliton molecules in a passively mode-locked erbium-doped fiber laser experimentally in 2001 [4]. Whereafter, in 2005, Stratmann et al. presented the demonstration of temporal soliton molecules in a dispersion-managed fiber [3]. In recent years, with the diversification of new mode-locking materials, the blowout type growth of new soliton effects has been observed in passively mode-locked fiber lasers based on saturable absorbers (SAs) such as carbon nanotubes (CNTs) [5], graphene [6], black phosphorus (BP) [7] and molybdenum disulfide (MoS$_2$) [8]. In 2012, Gui et al. experimentally obtained the in-phase soliton pairs in fiber lasers [9]. Soon afterward, their group achieved the wavelength-tunable soliton molecules in a fiber laser [14] and discovered quantized pulse separations between phase-locked soliton pairs in a thulium-doped fiber laser for the first time [10]. In 2020, Song et al. measured the timing jitter inner soliton molecules [11], and then found the intra-molecular timing jitter has a quantum origin [12]; in 2022, they further investigated the way to precisely control the oscillation frequencies in the soliton molecules [13].

Although these pioneering works have laid a solid foundation for the further investigation of soliton molecules, we find that the reported mode-locked soliton molecules have a common problem of pulses with low SNR. In practical applications, especially in the fiber communication system, lower SNR will result in the signal transmission and processing inefficiency.

Table I lists the SNRs and the related key parameters in works on soliton molecules that ever reported over the last decade. The low SNR of soliton molecules will potentially block the applications of soliton molecules laser in channel capacity improvement to some degree. Thus, the exploration solitons generation is of great significance.

In this work, we redesigned the oscillator structure by integrating a 7 nm narrow band pass filter in the cavity to filter out excess noise and improved the soliton pairs with superior SNR, even up to 80 dB. By appropriately adjusting the pump power and waveplates, the more complex soliton molecules with a composition of double-solitons, triple-solitons,quadruple-solitons, and quintuple-solitons bound states can be easily

TABLE I
THE CHARACTERISTICS OF SOLITON MOLECULES THAT
HAVE BEEN REPORTED

Year	SAs	Central wavelength (nm)	Repetition rate (MHz)	SNR (dB)	Ref.
2016	NPR	1926.1	42.19	60	[14]
2016	BPQDs	1568.5	15.15	64	[15]
2018	Graphene	1560	19.5	60	[16]
2018	MoS$_2$	1931.5	66.57	56	[2]
2018	NCF-GIMF	1573.72	16.63	74	[17]
2019	NPR	1953.1	104	58	[18]
2020	NPR	1555	87	70	[19]
2022	NPR	1970.2	47.76	80	This work

Notes: BPQDs: black phosphorus quantum dots; NCF-GIMF: hybrid no-core fiber-graded index multimode fiber.
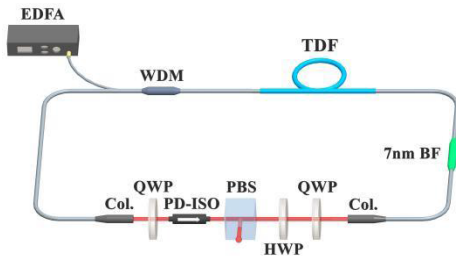

Fig. 1. The schematic of the laser experimental setup. EDFA: erbium-doped fiber amplifier; WDM: wavelength division multiplexer; TDF: Tm-doped fiber; PD-ISO: polarization-dependent isolator; QWP: quarter-wave plate; HWP: half-wave plate; PBS: polarization beam splitter; Col.: collimator; 7 nm BF: 7-nm bandpass filter.

realized. On this basis, we also systematically analyzed the spectral and temporal characteristics of multiple soliton molecules at different pumping powers, and found that decrease of pulse energy will result in a reduction of the number of solitons within the molecules. Finally, we also have experimentally confirmed the theoretical results on how the group velocity dispersion (GVD) and third-order dispersion (TOD) in the cavity can affect the soliton molecules.

II. EXPERIMENTAL SETUP AND RESULTS

Figure 1 shows the schematic of the experimental setup. The oscillator is constituted by an 18 cm-long high Tm-doped fiber (TDF, Nufern SM-TSF-5/125), an NPR structured polarization tuning mechanism consisting by half waveplates, a polarization beam splitter (PBS), and two quarter waveplates; a polarization-dependent isolator (PD-ISO) is used to guarantee the unidirectional operation of the ring cavity. The system is pumped by an erbium-doped CW fiber laser (EDFL) operating at 1560 nm with the maximum output power of 3 W. A 1560/1970 nm wavelength division multiplexer (WDM) is used for cavity power coupling. The GVD of the TDF and SMF-28e at 2 μm is -0.045 ps^2/m and -0.071 ps^2/m, respectively; the total cavity length is around 4.5 m, while counting in the device's pigtails and free space parts; the net anomalous dispersion in cavity is estimated to be -0.279 ps^2. To simplify the cavity structure, the PBS reflection beam is used as the energy output port for monitoring. The mode-locking pulse
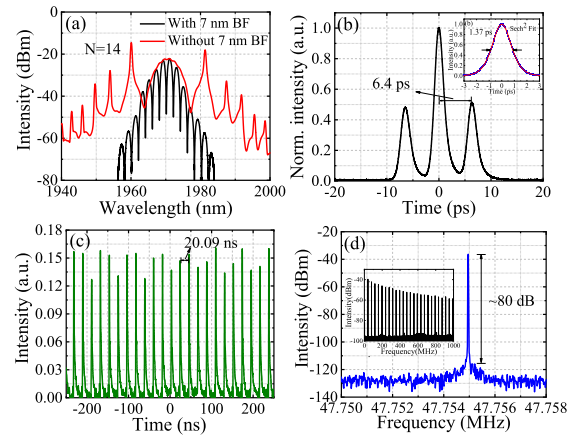

Fig. 2. (a) Optical spectrum with 7 nm BF and without 7 nm BF. (b) Autocorrelation trace of the soliton pairs. (c) Oscilloscope trace. (d) RF spectrum, inset: RF spectrum in a scanning range of 1 GHz.

repetition rate is detected by a 2.5-GHz digital oscilloscope (OSC, Yokogawa DLM2054). The output spectrum is measured by a spectrum analyzer (OSA, Yokogawa AQ6375) with a resolution of 0.02 nm. Besides, an intensity autocorrelator (Femtochrome, FR-103XL) is employed to measure the pulse duration and the temporal separation.

A stable conventional self-starting soliton mode-locking is realized by appropriately adjusting the waveplate at the pump power of 0.902 W. To get a simple molecule with two solitons, we slightly increase the pump power and optimize the system parameters simultaneously, the output characteristics of the soliton pairs are presented in Fig. 2. A comparison of the mode-locked pulse spectra in conditions of with and without 7 nm BF in cavity is presented in this figure. Because of the insertion of the BF, it's obviously that the pulse spectrum is narrowed in both long and short wavelength; the spectral Kelly sidebands are tightened and is replaced by a series of 14 (N) interference fringes with a high-contrast modulation period of 2.08 nm. According to the definition of the soliton phase in reference [9], one can confirm that the phase difference between the two mode-locked solitons is around $-\pi/2$. Fig. 2(b) shows the soliton pairs autocorrelation traces. As can be seen that there are three peaks contained in the molecule, symmetrically distributed, and the separations are measured nearly 6.4 ps. The durations of them are almost the same, nearly 1.37 ps, while fitted by a sech^2 profile. The intensity ratio is measured as 1:2:1, indicating that the soliton pairs have identical intensity and pulse duration. Fig. 2(c) shows the pulse period is 20.09 ns. Fig. 2(d) shows the measured SNR of the soliton pairs, which is as high as 80 dB with 10 Hz resolution bandwidth and 1 GHz span at a fundamental repetition rate of 47.76 MHz; which means the mode-locking state with high stability.

In Fig. 3, the blue dashed line shows the variation of pulse separation with the changes of fringes N in the spectrum via tuning the angle of the waveplates. The corresponding SNR is also measured, as shown in the black dashed line. The temporal separation and the number of spectral interference fringes are positively correlated. The linear fitting result shows that the time interval increased by 0.54 ps for each additional N. Even if the pulse space distributions increase, the SNR
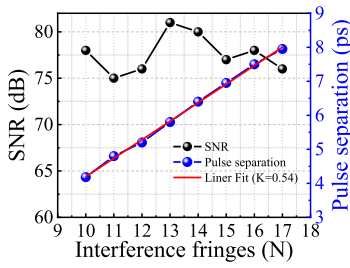
Fig. 3.   SNR (black line) and pulse separation (blue line) correspond to different interference fringes (N) of the soliton pairs.
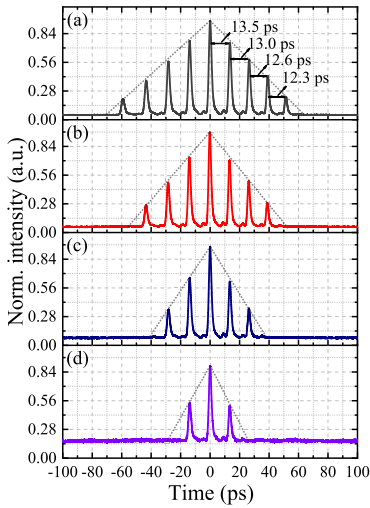

Fig. 4.   Autocorrelation trace of five (a), four (b), three (c), and two (d) soliton molecules.
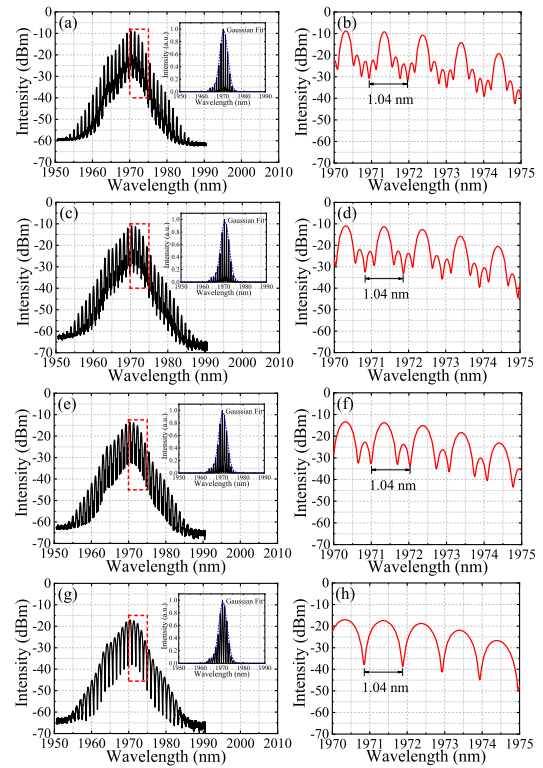

Fig. 5.   Measured spectra of various soliton molecules. (a), (c), (e), (g) optical spectrum of five, four, three, two soliton molecules, inset: the linear spectrum; (b), (d), (f), (h) the enlarged optical spectra of five, four, three, two soliton molecules.

remains at a high level, all above 75 dB. This may be helpful to the novel technique proposed in recent years of controlling bound state soliton pairs at separated intervals by machine vision with high signal stability [20].

On this basis, we continue to explore the temporal and spectral characteristics of the pump power variation. By precisely scaling the pump power, we can obtain a series of soliton molecules containing different solitons, indicating that soliton numbers are greatly affected by intracavity nonlinearity. The temporal characteristics are measured, as seen in Fig. 4. We can see that with the increase of pump power, many new members appeared, which are equally spaced and symmetrically distributed. Fig. 4(a) shows the five soliton molecules generated at the pump power of 1.313 W. The autocorrelation trace shows an intensity ratio of 1:2:3:4:5:4:3:2:1, following a linear distribution. However, due to the precision of the autocorrelator and imperfections in measurement, there is a slight deviation in the distance between pulses. With the reduction of the pump power, it's fascinating that the sidebands are reduced regularly, but their separation remains unchanged. Fig. 4(b)-(d) are soliton molecules measured at a pump power of 1.256 W, 1.119 W, and 0.998 W. The five soliton molecules degenerate into four, three, and two soliton molecules, respectively. In this situation, there is not enough energy supplied to the pulses, resulting in a decrease in the number of solitons within the bound states. However, since the remaining pulses maintain the same phase difference [17], the pulse width and separation of these solitons in the molecule are remain unchanged.

Figure. 5 presents the corresponding spectra of each soliton molecules mentioned above in Fig. 5(a), (c), (e), (g), respectively. One can see that the overall spectral in logarithmic and linear coordinates are nearly follow a Gaussian distribution; the fringes in each spectrum are clearly presented but difficult to be precisely measured. To further observe the detailed evolution of each spectrum, we partially enlarged the spectra, as is shown in Fig. 5 (b), (d), (f), (h), on the right side of each spectrum. Thus, we can clearly view the humps between the two interference fringes, and the distance between them can also be precisely measured. The spectra are characterized by a district and regular periodic structure on the enlarged spectra. In comparing with those spectra, and the number of humps is related to the number of solitons in each molecule. The distance between the deepest valleys of the fringes in spectrum are equally spaced, this value is measured as 1.04 nm. The same modulation period suggests that multiple soliton molecules, as well as soliton pairs, follow the equation $\Delta T = \lambda_0^2/(c \times \Delta\lambda)$, where ΔT represents the pulse separation, c is the light speed in vacuum, $\lambda 0$ is the central wavelength, and $\Delta\lambda$ is the modulation period of the optical spectrum [19].

We also measured the variation of SNR, output power, peak width and peak power of those soliton molecules with soliton number, as is shown in Fig. 6. The SNR of the five soliton molecules to the two soliton molecules is 70 dB, 80 dB, 66 dB, and 75 dB, respectively. The average power of the output pulse does not follow linearly with the number of solitons, which indicates that the energy of the soliton molecules is not a simple superposition of the energy of several solitons, this conclusion was also drawn and mentioned in reference [18].
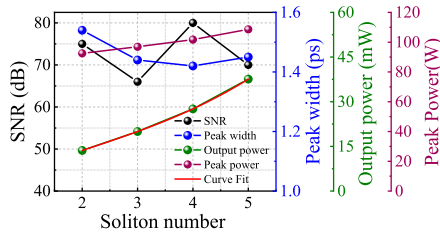
Fig. 6. SNR (black line), peak width (bule line), peak power (grey line) and output power (green line) of various soliton molecules.

TABLE II
THE VARIATONS OF LASER OUTPUT PULSE PERFORMANCES
WITH SMF-28E FIBER LENGTH

Fiber length (m)	GVD (ps²/m)	TOD (ps³/m)	Min interference fringes (N)	Max modulation period (nm)	Pulse separation (ps)
0	-0.279	4.37×10^{-4}	10	3.10	4.2
1	-0.350	5.41×10^{-4}	13	2.43	5.6
2	-0.421	6.45×10^{-4}	14	2.30	5.8

Besides, to explore how the dispersion in cavity can affect the characteristics of the soliton molecules, we optimized the cavity dispersion by introducing some SMF-28e fiber into the laser cavity. The description of the soliton pairs evolution at different distributions is given in Table II. As can be seen from the listed data that with the increase of GVD and TOD, the maximum modulation period of the soliton pairs is decreasing, which means the minimum distance between the solitons is rising. This experimental result is a powerful proof to the theoretical work in reference [21] on solitons characteristics variation with dispersion in oscillator.

III. CONCLUSION

In conclusion, we report a detailed exploration on the stationary soliton molecules generation and its properties modulation in a Tm-doped fiber-based NPR mode-locked fiber laser oscillator. The main work includes the soliton molecules SNR improvement, pulse separation controlling, soliton spectral analysis, and the exploration on how dispersion can affect the solitons. All this exploration work is done to obtain soliton molecules that can be more effectively applied to telecommunication systems. On this basis, we will further focus on studying the physical regimes and dynamics of the soliton molecules by using the dispersive Fourier-transform (DFT) measurement technique in the near future.

REFERENCES

[1] P. Grelu and N. Akhmediev, "Dissipative solitons for mode-locked lasers," *Nature Photon.*, vol. 6, no. 2, pp. 84–92, Feb. 2012.

[2] P. Wang et al., "Self-organized structures of soliton molecules in 2-μm fiber laser based on MoS$_2$ saturable absorber," *IEEE Photo. Technol. Lett.*, vol. 30, no. 13, pp. 1210–1213, Jul. 2018.

[3] M. Stratmann, T. Pagel, and F. Mitschke, "Experimental observation of temporal soliton molecules," *Phys. Rev. Lett.*, vol. 95, no. 14, Sep. 2005, Art. no. 143902.

[4] D. Y. Tang, W. S. Man, H. Y. Tam, and P. D. Drummond, "Observation of bound states of solitons in a passively mode-locked fiber laser," *Phys. Rev. A, Gen. Phys.*, vol. 64, no. 3, 2001, Art. no. 033814.

[5] H. H. Liu and K. K. Chow, "High fundamental-repetition-rate bound solitons in carbon nanotube-based fiber lasers," *IEEE Photon. Technol. Lett.*, vol. 27, no. 8, pp. 867–870, Apr. 15, 2015.

[6] L. Gui, X. Li, X. Xiao, H. Zhu, and C. Yang, "Widely spaced bound states in a soliton fiber laser with graphene saturable absorber," *IEEE Photon. Technol. Lett.*, vol. 25, no. 12, pp. 1184–1187, May 13, 2013.

[7] Y. Song et al., "Vector soliton fiber laser passively mode locked by few layer black phosphorus-based optical saturable absorber," *Opt. Exp.*, vol. 24, no. 23, pp. 25933–25942, 2016.

[8] Y. Wang et al., "Harmonic mode locking of bound-state solitons fiber laser based on MoS$_2$ saturable absorber," *Opt. Exp.*, vol. 23, no. 1, pp. 205–210, 2015.

[9] L. Gui, X. Xiao, and C. Yang, "Observation of various bound solitons in a carbon-nanotube-based erbium fiber laser," *J. Opt. Soc. Amer. B, Opt. Phys.*, vol. 30, no. 1, p. 158, Jan. 2013.

[10] P. Wang, X. Xiao, and C. Yang, "Quantized pulse separations of phase-locked soliton molecules in a dispersion-managed mode-locked Tm fiber laser at 2 μm," *Opt. Lett*, vol. 42, no. 1, pp. 29–32, 2017.

[11] Y. Song et al., "Attosecond timing jitter within a temporal soliton molecule," *Optica*, vol. 7, no. 11, pp. 1531–1534, 2020.

[12] D. Zou, Z. Li, P. Qin, Y. Song, and M. Hu, "Quantum limited timing jitter of soliton molecules in a mode-locked fiber laser," *Opt. Exp.*, vol. 29, no. 21, pp. 34590–34598, 2021.

[13] D. Zou et al., "Synchronization of the internal dynamics of optical soliton molecules," *Optica*, vol. 9, no. 11, pp. 1307–1313, 2022.

[14] P. Wang, C. Bao, B. Fu, X. Xiao, P. Grelu, and C. Yang, "Generation of wavelength-tunable soliton molecules in a 2-μm ultrafast all-fiber laser based on nonlinear polarization evolution," *Opt. Lett*, vol. 41, no. 10, pp. 2254–2257, 2016.

[15] Z. Wang et al., "Black phosphorus quantum dots as an efficient saturable absorber for bound soliton operation in an erbium doped fiber laser," *IEEE Photon. J.*, vol. 8, no. 5, pp. 1–10, Oct. 2016.

[16] L. Gui and C. Yang, "Soliton molecules with $\pm\pi/2,0,$ and π phase differences in a graphene-based mode-locked erbium-doped fiber laser," *IEEE Photon. J.*, vol. 10, no. 3, pp. 1–9, Jun. 2018.

[17] T. Zhu, Z. Wang, D. N. Wang, F. Yang, and L. Li, "Observation of controllable tightly and loosely bound solitons with an all-fiber saturable absorber," *Photon. Res.*, vol. 7, no. 1, pp. 61–68, 2018.

[18] R. Liu et al., "Formation of various soliton molecules in a 2-μm anomalous-dispersion mode-locked fiber laser," *IEEE Photo. Technol. Letter.*, vol. 31, no. 5, pp. 341–344, Mar. 2019.

[19] D. Zou, Y. Zhang, Y. Song, and M. Hu, "Sub-100 fs bound state solitons and period-doubling bifurcations in a mode-locked fiber laser," *IEEE Photon. Technol. Lett.*, vol. 32, no. 20, pp. 1311–1314, Oct. 15, 2020.

[20] J. Girardot, A. Coillet, M. Nafa, F. Billard, E. Hertz, and P. Grelu, "On-demand generation of soliton molecules through evolutionary algorithm optimization," *Opt. Lett.*, vol. 47, no. 1, pp. 134–137, 2022.

[21] H. Sakaguchi, D. V. Skryabin, and B. A. Malomed, "Stationary and oscillatory bound states of dissipative solitons created by third-order dispersion," *Opt. Lett.*, vol. 43, no. 11, pp. 2688–2691, 2018.